Journal of Fluorine Chemistry 131 (2010) 907–914

Contents lists available at ScienceDirect

Journal of Fluorine Chemistry

journal homepage: www.elsevier.com/locate/fluor

# Hydroxylammonium fluorometalates: Synthesis and characterisation of a new fluorocuprate and fluorocobaltate

Matjaž Kristl [a,*], Brina Dojer [a], Marta Kasunič [b], Amalija Golobič [b], Zvonko Jagličić [c], Miha Drofenik [a,d]

[a] University of Maribor, Faculty of Chemistry and Chemical Engineering, Smetanova 17, SI-2000 Maribor, Slovenia
[b] University of Ljubljana, Faculty of Chemistry and Chemical Technology, Aškerčeva 5, SI-1000 Ljubljana, Slovenia
[c] Institute of Mathematics, Physics and Mechanics and Faculty of Civil and Geodetic Engineering, University of Ljubljana, Jadranska 19, SI-1000 Ljubljana, Slovenia
[d] Jožef Stefan Institute, Jamova 39, SI-1000 Ljubljana, Slovenia

ARTICLE INFO

*Article history:*
Received 2 April 2010
Received in revised form 4 June 2010
Accepted 8 June 2010
Available online 15 June 2010

*Keywords:*
Cuprate
Cobaltate
Fluorides
X-ray diffraction
Hydrogen bond

ABSTRACT

The first layered hydroxylammonium fluorometalates, $(NH_3OH)_2CuF_4$ and $(NH_3OH)_2CoF_4$, were prepared by the reaction of solid $NH_3OHF$ and the aqueous solution of copper or cobalt in HF. Both compounds crystallize in monoclinic, $P2_1/c$, unit cell with parameters: $a = 7.9617(2)$ Å, $b = 5.9527(2)$ Å, $c = 5.8060(2)$ Å, $\beta = 95.226(2)^\circ$ for $(NH_3OH)_2CuF_4$ and $a = 8.1764(3)$ Å, $b = 5.8571(2)$ Å, $c = 5.6662(2)$ Å, $\beta = 94.675(3)^\circ$ for $(NH_3OH)_2CoF_4$, respectively. Magnetic susceptibility was measured between 2 K and 300 K giving the effective Bohr magneton number of 2.1 for Cu and 5.2 BM for Co. At low temperatures both complexes undergo a transition to magnetically ordered phase. The thermal decomposition of both compounds was studied by TG, DSC and X-ray powder diffraction. The thermal decomposition of $(NH_3OH)_2CuF_4$ is a complex process, yielding $NH_4CuF_3$ as an intermediate product and impure $Cu_2O$ as the final residue, while $(NH_3OH)_2CoF_4$ decomposes in two steps, obtaining $CoF_2$ after the first step and CoO as the final product.



## 1. Introduction

Hydroxylammonium fluorometalates with a general formula $(NH_3OH)_xMF_y$ are interesting for the study of hydrogen bonds, since they include all three elements that are capable to form strong hydrogen bonds (O, N and F). Although the first hydroxylammonium fluorometalates (M = Si, Ti) were reported in 1908 by Ebler and Schott [1], until 1990 only three new compounds (M = U, Th) were reported [2,3]. Since the early 90s, our laboratory has reported on the synthesis and properties of a number of new hydroxylammonium fluorometalates of main group elements (M = Al, Ga, In, Si, Ge) [4–9] and transition metals (M = Ti, Zr, Hf, Cr, V) [10–14]. The main advantage of our method is the use of solid $NH_3OHF$, prepared by adding an ethanol solution of $NH_2OH$ to an aqueous solution of hydrofluoric acid [15], instead of aqueous or ethanolic hydroxylammonium solutions used by earlier researchers. To the best of our knowledge, no reports about hydroxylammonium fluorocuprates and -cobaltates have been published, so we decided to study reactions in the systems $NH_3OHF$–Cu–HF (aq) and $NH_3OHF$–Co–HF (aq). The main aim of the work was to fulfill the inorganic systematics in the field of interest.

Since the chemistry of hydroxylammonium is analogous to that of ammonium and hydrazinium, we also reviewed publications reporting fluorocuprates and -cobaltates of ammonium and hydrazinium. Ammonium fluoride complexes, $NH_4CoF_3$ and $NH_4CuF_3$, have been known long ago [16] while $(NH_4)_2MF_4$ type compounds (M = Co, Cu, Ni), isostructural with $K_2NiF_4$, have been reported by Crocket and Grossman [17]. Later, Troyanov et al. [18,19] also reported on the synthesis and crystal structure of three ammonium fluorocuprates, $NH_4CuF_3$, $(NH_4)_2CuF_4$ and $(NH_4)_2CuF_4{\cdot}2H_2O$. Siebert and Breitenstein [20] obtained $[Co(NH_3)_6]CoF_6$ by the thermal decomposition of $[Co(NH_3)_6]F_3$ and determined its crystal structure whereas the synthesis and structural assessment of hydrazinium fluorocobaltate, $(N_2H_4)_2CoF_2{\cdot}2H_2O$, has been reported by Bhattacharjee et al. [21].

## 2. Results and discussion

### 2.1. Thermogravimetrical results

**(a)** The thermal decomposition of the new blue compound with a formula $(NH_3OH)_2CuF_4$ is shown in Fig. 1. The new compound is stable up to 353 K and decomposes in five partially overlapping steps. In the first step up to 453 K the sample loses 19.3% of its mass. The DSC curve shows a significant exothermic peak at this temperature. From 453 K to 523 K the mass is falling quite fast. Up to 523 K the sample loses 36.9% of its starting mass. At the end of the third temperature interval at 553 K the mass loss amounts to 41.0% and at 673 K 45.7%. Finally, at 1273 K 58.2% of the initial weight is lost.

* Corresponding author. Tel.: +386 2 22 94 415; fax: +386 2 25 27 774.
*E-mail address:* matjaz.kristl@uni-mb.si (M. Kristl).

0022-1139/$ – see front matter © 2010 Elsevier B.V. All rights reserved.
doi:10.1016/j.jfluchem.2010.06.004

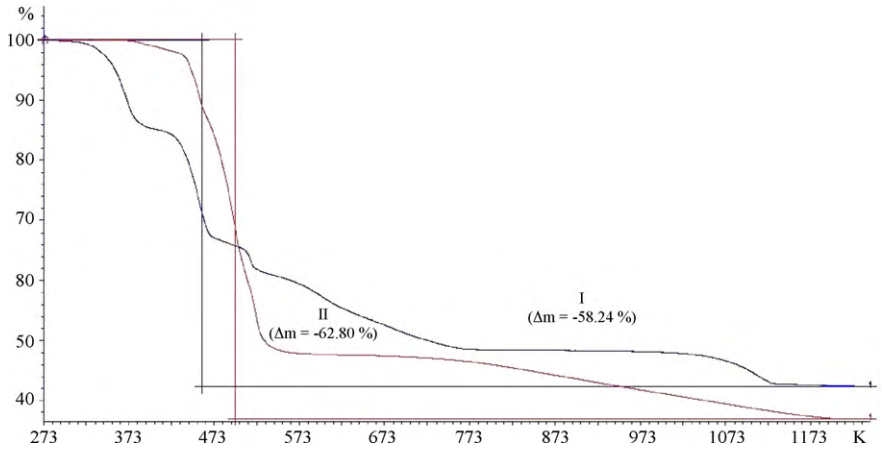


**Fig. 1.** Thermogravimetric analysis of $(NH_3OH)_2CuF_4$ (I) and $(NH_3OH)_2CoF_4$ (II).

The room temperature X-ray powder diffraction patterns are shown in Fig. 2. At 453 K, after the first significant decomposition step, the diffraction pattern shows that the prevalent product is $NH_4CuF_3$ with some traces of $CuF_2{\cdot}2H_2O$. At 523 K, traces of four compounds are present: $NH_4CuF_3$, $Cu_2OHF_3$, $CuF_2{\cdot}2H_2O$ and CuO. Besides CuO, there are also some traces of $Cu_2OHF_3$, $CuF_2$ and CuOHF present at 673 K. At 873 K the prevalent products are $CuF_2$, CuOHF and CuO. The final residue of the compound at 1273 K is $Cu_2O$ with some traces of CuO.

The proposed parallel chemical reactions taking place during the thermal decomposition of $(NH_3OH)_2CuF_4$ could be described by following equations (first step):

$$3(NH_3OH)_2CuF_4 \rightarrow 3CuF_2{\cdot}2H_2O + 6HF + 2NH_3 + 2N_2$$

$$3(NH_3OH)_2CuF_4 \rightarrow NH_4CuF_3 + Cu_2OHF_3 + 2N_2 + NH_3 + 5H_2O + 6HF$$

Second step:

$$Cu_2OHF_3 \rightarrow CuOHF + CuF_2$$

$$Cu_2OHF_3 \rightarrow CuO + CuF_2 + HF$$

$$CuOHF \rightarrow CuO + HF$$

Final step:

$$CuF_2 + H_2O \rightarrow CuO + 2HF$$

$$2CuO \rightarrow Cu_2O + 1/2O_2$$

**(b)** The thermal decomposition of the new violet crystal compound with a formula $(NH_3OH)_2CoF_4$ in a nitrogen atmosphere is shown in Fig. 1. The TG curve shows two general decomposition steps. The first initial drift on the curve can be attributed to the loss of adsorbed water and HF. Up to 573 K the sample loses 51.4% of its starting mass while at 1173 K, 62.8% of the initial mass is lost and the mass of the residue does not change anymore. The products of the thermal decomposition at different temperatures and the final residue were identified by X-ray powder diffraction. The diffraction patterns are shown in Fig. 3. At 573 K, after the first significant decomposition step, the diffraction pattern shows that the prevalent product is $CoF_2$ and the same product is also present at 773 K. At 973 K the prevalent product of the decomposition is still $CoF_2$ with some traces of CoO. The final residue at 1273 K is CoO. The measured mass loss in the first step ($\Delta m_{meas}/m$ = 51.4%) is in good agreement with the value, calculated for the decomposition to $CoF_2$ ($\Delta m_{calc}/m$ = 52.2%):

$$3(NH_3OH)_2CoF_4 \rightarrow 3CoF_2 + 6HF + 2NH_3 + 2N_2 + 6H_2O$$

The second decomposition step can be described by the reaction:

$$CoF_2 + H_2O \rightarrow CoO + 2HF$$

The measured mass loss for both decomposition steps ($\Delta m_{meas}/m$ = 62.8%) is also in good agreement with the calculated value ($\Delta m_{calc}/m$ = 63.0%).

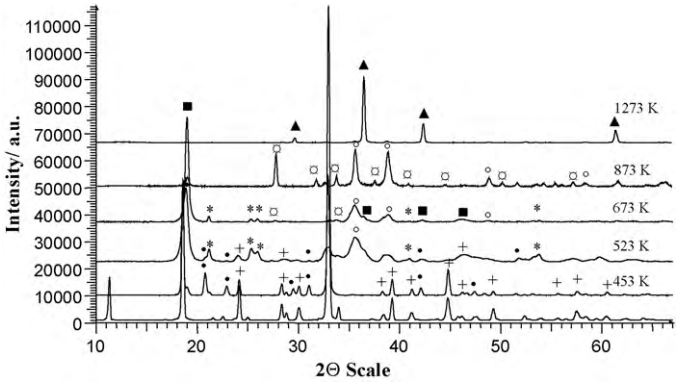


**Fig. 2.** X-ray diffraction patterns of $(NH_3OH)_2CuF_4$ (lowest) and the products of thermal decomposition at different temperatures: (+)$CuF_2{\cdot}2H_2O$ (PDF 000-25-0276), (●)$NH_4CuF_3$ (PDF 000-24-1105), (*)$Cu_2OHF_3$ (PDF 000-06-0170), (○)$CuF_2$ (PDF 010-70-1936), (°) CuO (PDF 010-70-6827), (■) CuOHF (PDF 000-07-0306), (▲) $Cu_2O$ (PDF 000-05-0667).

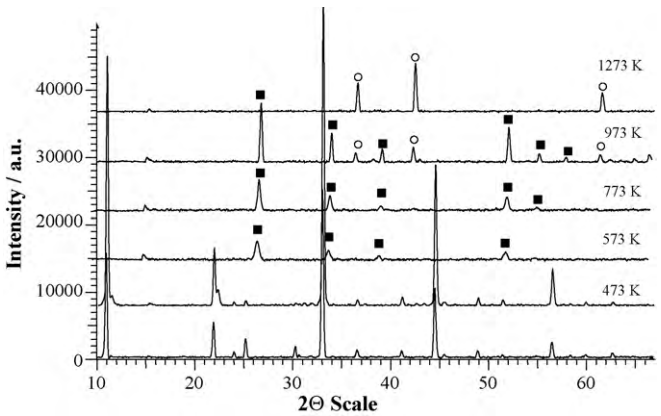


**Fig. 3.** X-ray diffraction patterns of $(NH_3OH)_2CoF_4$ (lowest) and the products of thermal decomposition at different temperatures: (■) $CoF_2$ (PDF 000–33-0417), (○) CoO (PDF 000-48-1719).

**Table 1**
Fractional coordinates and equivalent displacement parameters (Å$^2$) for $(NH_3OH)_2CuF_4$ and $(NH_3OH)_2CoF_4$.

| | *x*/*a* | *y*/*b* | *z*/*c* | $U_{eq}$ |
|---|---|---|---|---|
| Cu | 0 | 1/2 | 1/2 | *0.01227(16) |
| F1 | 0.02524(12) | 0.26164(14) | 0.18853(15) | *0.0207(4) |
| F2 | 0.24256(10) | 0.54649(16) | 0.53460(14) | *0.0197(4) |
| N | 0.2773(2) | 0.4955(2) | 0.0166(2) | *0.0182(7) |
| O | 0.40411(15) | 0.4346(2) | 0.1923(2) | *0.0257(5) |
| H1 | 0.259(4) | 0.637(5) | 0.016(5) | 0.028(5) |
| H2 | 0.178(4) | 0.427(5) | 0.035(5) | 0.034(6) |
| H3 | 0.321(3) | 0.460(5) | −0.118(5) | 0.027(5) |
| H4 | 0.359(5) | 0.461(6) | 0.318(6) | 0.046(7) |
| Co | 0 | 1/2 | 1/2 | *0.0125(2) |
| F1 | 0.02632(12) | 0.28136(16) | 0.21868(15) | *0.0214(4) |
| F2 | 0.24696(12) | 0.55023(18) | 0.53674(17) | *0.0213(4) |
| N | 0.28271(17) | 0.4920(3) | 0.0182(3) | *0.0196(7) |
| O | 0.40407(16) | 0.4206(3) | 0.1948(2) | 0.0257(5) |
| H1 | 0.260(4) | 0.627(8) | 0.036(6) | 0.029(7) |
| H2 | 0.196(4) | 0.424(5) | 0.049(5) | 0.017(5) |
| H3 | 0.312(5) | 0.472(7) | −0.109(9) | 0.033(7) |
| H4 | 0.340(4) | 0.467(6) | 0.337(6) | 0.026(6) |

*$U = U_{eq} = 1/3\sum_i\sum_j U_{ij} a_i^* a_j^* a_i a_j$.

### 2.2. Characterisation and crystal structure of $(NH_3OH)_2CuF_4$ and $(NH_3OH)_2CoF_4$

The atomic coordinates and equivalent displacement parameters are given in Table 1. Bond lengths and angles can be found in Table 2. The fundamental building units of isostructural compounds $(NH_3OH)_2CuF_4$ and $(NH_3OH)_2CoF_4$ are $NH_3OH^+$ cations and $MF_6$ octahedra in which the metal ion lies on the inversion centre, as can be seen in Fig. 4. In $(NH_3OH)_2CuF_4$, $CuF_6$ octahedra are elongated (Cu–F distances in the basal plane of the octahedra are from 1.904(1) Å to 1.943(1) Å and the axial ones are 2.322(1) Å) due to non-symmetrical occupation of $e_g$ orbitals known as Jahn–Teller effect, which is typical for $Cu^{2+}$ compounds. The $CoF_6$ octahedra in $(NH_3OH)_2CoF_4$ are less distorted. All Co–F bond distances range from 2.034(1) Å to 2.070(1) Å.

In both compounds each of $MF_6$ octahedra shares four of its vertices in a way that each vertex is shared between two octahedra. The result of the described connecting is the formation of a two-dimensional structure with $[MF_4^{2-}]_n$ layers that are perpendicular to *a* edge. Fig. 5 shows $CuF_6$ octahedra connections into layer and stacking of such layers in $(NH_3OH)_2CuF_4$. Connectivity of octahedra in $(NH_3OH)_2CoF_4$ is the same.

**Table 2**
Bond lengths (Å) and angles (°) of the title compounds.

| $(NH_3OH)_2CuF_4$ | | $(NH_3OH)_2CoF_4$ | |
|---|---|---|---|
| Cu–F(1) | 2.322(1) | Co–F(1) | 2.070(1) |
| Cu–F(2) | 1.943(1) | Co–F(2) | 2.034(1) |
| Cu–F(1)$_{-x,\ 1/2+y,\ -z+1/2}$ | 1.904(1) | Co–F(1)$_{-x,\ 1/2+y,\ -z+1/2}$ | 2.063(1) |
| O–N | 1.416(2) | O–N | 1.414(2) |
| O–H(4) | 0.86(4) | O–H(4) | 1.03(3) |
| N–H(1) | 0.86(3) | N–H(1) | 0.82(5) |
| N–H(2) | 0.91(3) | N–H(2) | 0.84(3) |
| N–H(3) | 0.91(3) | N–H(3) | 0.79(5) |
| F(1)–Cu–F(2) | 90.68(3) | F(1)–Co–F(2) | 90.21(4) |
| N–O–H(4) | 104(3) | N–O–H(4) | 95.9(19) |
| O–N–H(1) | 111(2) | O–N–H(1) | 111(2) |
| O–N–H(2) | 111.9(2) | O–N–H(2) | 106(2) |
| O–N–H(3) | 104.9(2) | O–N–H(3) | 111(3) |

Bond lengths in $MF_6$ octahedra in both compounds are in good agreement with literature data of compounds with similar connectivity yielding $[MF_4^{2-}]_n$ layers where bond lengths from 1.864(5) Å to 2.275(5) Å for copper compounds [22–26], and from 2.025(3) Å to 2.075(1) Å for cobalt compounds are reported [27,28]. In cobalt compounds Co–F(terminal) bond lengths are in all cases slightly shorter than Co–F(bridging) ones. This is not always the case in copper compounds due to Jahn–Teller distortion of octahedra. The N–O distances, 1.416(2) Å and 1.414(2) Å, are similar in both compounds and are in accordance with previously reported values [5–8,11,13,29] for other hydroxylammonium fluorometalates, which range from 1.396(2) Å to 1.414(2) Å.

When considering only the exchange of cobalt ion with the smaller copper one (corresponding ionic radii for octahedral coordination are 0.73 Å for Cu and 0.745 Å for Co in high-spin compounds, respectively), the reduction of all three cell edges would be expected. But due to the elongation of $CuF_6$ octahedra in approximately diagonal direction between *b* and *c* edges, the elongation of the latter two edges occurs and only the edge *a* reduces.

The aforementioned $[MF_4^{2-}]_n$ layers are connected via $NH_3OH^+$ cations positioned in between the anionic layers through strong hydrogen bonds of two types (O–H...F and N–H...F) whose geometry is described in Table 3. All conclusions with regard to the strength of hydrogen bonds are made on the basis of geometrical parameters of these bonds, assuming that the shorter a distance between donor and acceptor is, the stronger such hydrogen bond is. The strongest hydrogen bond in both compounds is donated by

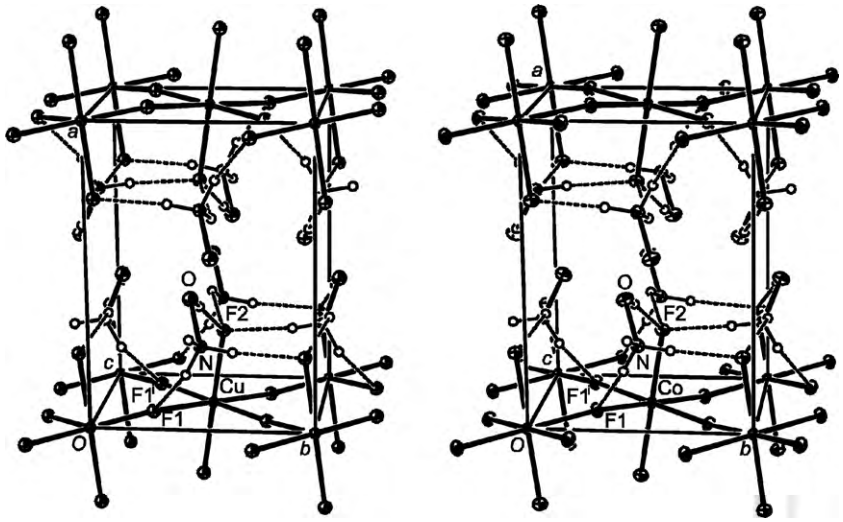


**Fig. 4.** ORTEP-3 view of structures of $(NH_3OH)_2CuF_4$ and $(NH_3OH)_2CoF_4$. Ellipsoids are drawn at 25% probability level. (i): $-x, 1/2 + y, 1/2 - z$; Dashed lines represent hydrogen bonds.

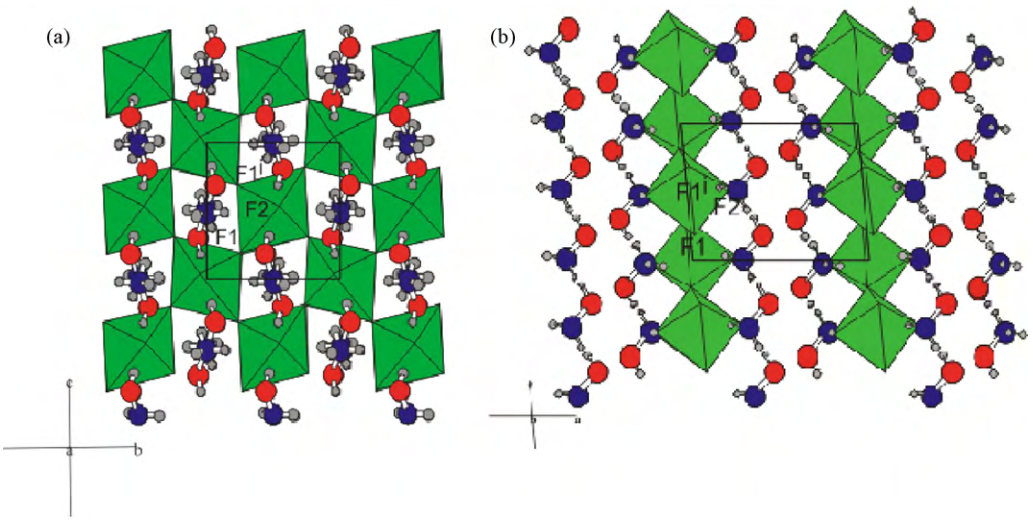


**Fig. 5.** A polyhedral representation of structure of $(NH_3OH)_2CuF_4$. (a) As viewed along *a* axis – presenting $CuF_6$ octahedra connections into fluorocuprate layer. (b) As viewed along *b* axis – showing the stacking of layers along *a* axis.

**Table 3**
Hydrogen bond lengths (Å) and angles (°) in $(NH_3OH)_2CuF_4$ (upper) and $(NH_3OH)_2CoF_4$ (lower part of the table).

| A–H...B | Distance A–B | Distance A–H | Distance B–H | Angle A–H...B | Symmetry operations of B |
|---|---|---|---|---|---|
| O–H(4)...F(2) | 2.552(1) | 0.86(4) | 1.71(4) | 169(4) | *x*, *y*, *z* |
| N–H(1)...F(2) | 2.743(2) | 0.86(3) | 1.89(3) | 174(3) | *x*, 3/2 − *y*, −1/2 + *z* |
| N–H(2)...F(1) | 2.707(2) | 0.91(3) | 1.86(3) | 156(3) | *x*, *y*, *z* |
| N–H(3)...F(2) | 2.803(1) | 0.91(3) | 2.12(3) | 131(2) | *x*, *y*, −1 + *z* |
| N–H(3)...O | 2.939(2) | 0.91(3) | 2.35(2) | 122(2) | 1 − *x*, 1 − *y*, −*z* |
| N–H(1)...F(1) | 2.964(2) | 0.86(3) | 2.53(3) | 112(2) | −*x*, 1 − *y*, −*z* |
| N–H(2)...F(1) | 3.050(2) | 0.91(3) | 2.52(3) | 118(2) | *x*, 1/2 − *y*, −1/2 + *z* |
| O–H(4)...F(2) | 2.527(2) | 1.03(3) | 1.50(3) | 176(3) | *x*, *y*, *z* |
| N–H(1)...F(2) | 2.700(2) | 0.82(5) | 1.89(5) | 167(3) | *x*, 3/2 − *y*, −1/2 + *z* |
| N–H(2)...F(1) | 2.756(2) | 0.84(3) | 1.94(3) | 162(3) | *x*, *y*, *z* |
| N–H(3)...F(2) | 2.741(2) | 0.79(5) | 2.09(5) | 141(4) | *x*, *y*, −1 + *z* |
| N–H(3)...O | 2.963(2) | 0.79(5) | 2.49(4) | 120(4) | 1 − *x*, 1 − *y*, −*z* |
| N–H(1)...F(1) | 3.065(2) | 0.82(5) | 2.70(3) | 108(3) | −*x*, 1 − *y*, −*z* |
| N–H(2)...F(1) | 3.043(2) | 0.84(3) | 2.54(3) | 119(2) | *x*, 1/2 − *y*, −1/2 + *z* |

hydroxyl oxygen (2.552(1) Å and 2.527(2) Å in cuprate and cobaltate, respectively). The comparison with other known structures of hydroxylammonium fluorometalates shows that the formation of one-dimensional (i.e. chains in $(NH_3OH)_2ZrF_6$ and $(NH_3OH)_3ZrF_7$ [11]) or two-dimensional (i.e. layers in both title compounds) fluorometalates by sharing fluorine atoms has no significant influence on the strength of O–H...F hydrogen bond. In $(NH_3OH)_3InF_6$ [6], $(NH_3OH)_3CrF_6$ [13] and $(NH_3OH)_3GaF_6$ [5] with mononuclear anion where no bridging fluorine atoms are present, O–H...F hydrogen bonds are of similar strength as in above mentioned extended fluorometalates (all O...F contact distances are in the range between 2.5 Å and 2.6 Å). On the other hand, the structures of $(NH_3OH)_2(TiF_6)(H_2O)_2$ [6] and $(NH_3OH)_2(SiF_6)(H_2O)_2$ [8] illustrate the effect of crystal water incorporation which has a significant influence on the strength of hydrogen bonds. In these two mononuclear structures hydroxyl group of the cation acts as a donor of a weaker hydrogen bond which is accepted by oxygen atom of water molecules instead of fluorine atoms of anions resulting in a formation of longer O–H...O hydrogen bond (O...O contact distance is longer than 2.64 Å). Fluorine atoms are the acceptors of weak hydrogen bonds donated by water molecules (O...F contact distances are longer than 2.72 Å).

In both title compounds, the nitrogen atom of the cation is a donor of three moderately strong hydrogen bonds to fluorine atoms of the anion (N...F contact distances in range of 2.7–2.8 Å). There are two additional weaker stabilising N–H...F contacts and also one N–H...O between cations themselves (N...F and N...O contact distances in range 2.9–3.0). Similarly, in the above mentioned hydroxylammonium fluorometalates we find some moderately strong and some weak hydrogen bonds donated by N atom of the cation. The exception is $(NH_3OH)_2(SiF_6)(H_2O)_2$ [8] where all donor...acceptor contact distances from N–H...F or N–H...O hydrogen bonds are longer than 2.815 Å.

### 2.3. Magnetic properties

Magnetic properties have been investigated in a temperature interval from 300 K to 2 K and in magnetic field up to 5 T. The measured data in Figs. 6 and 7 are already corrected for the sample holder contribution and for temperature independent Larmor diamagnetism of core electrons obtained from Pascal's tables.

Inverse susceptibility plot for $(NH_3OH)_2CuF_4$ measured in $H = 100$ Oe (inset in Fig. 6a) shows a perfect linear temperature dependence in high-temperature region. Hence the susceptibility for $T > 150$ K was fitted with the Curie–Weiss law:

$$\chi = \frac{C}{T - \Theta}. \quad (1)$$

We obtained the Curie constant $C = 0.62$ emu K/mol and $\Theta = -18$ K. From the Curie constant $C$ the effective moment $\mu_{eff} = 2.1$ BM was calculated. This value is larger than expected for $Cu^{2+}$ spin-only value of 1.73 BM and is probably due to a spin–orbit coupling and is within the reported values for $Cu^{2+}$, which are within the range $\mu_{eff} = 1.8$–2.2 BM [30].

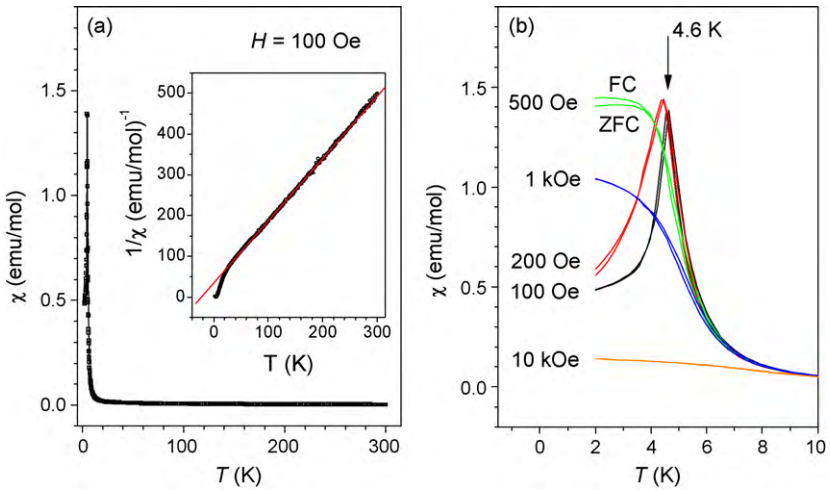


**Fig. 6.** (a) Susceptibility and inverse susceptibility (inset) as a function of temperature for Cu-sample. Full red line is the result of Curie–Weiss fit (Eq. (1)). (b) Susceptibilities measured in different magnetic fields. (For interpretation of the references to color in this figure legend, the reader is referred to the web version of the article.)

Negative Curie–Weiss temperature $\Theta = -18$ K from fit (1) indicates an antiferromagnetic interaction between nearest neighbour copper atoms. However, when susceptibility approaching 5 K it rapidly increases – showing a ferromagnetic ordering is established. The peak at 4.6 K (Fig. 6b) is followed by a sudden drop of $\chi(T)$. In order to get better insight into the magnetic properties of the complex we performed additional ZFC/FC susceptibility measurements in different magnetic fields as well as isothermal magnetization measurements $M(H)$ at temperatures above and below the 4.6 K. The ZFC (zero field cooling) run means that a sample was first cooled in zero magnetic field and susceptibility was measured on heating the sample in magnetic field. The FC (field cooled) run is the same as ZFC but the sample was cooled in magnetic field. In Fig. 6b susceptibilities for $H = 100$ Oe, 200 Oe, 500 Oe, 1 kOe and 10 kOe are shown only in low temperature region. The susceptibilities above 9 K are the same for all fields. We notice that there is only a small difference between ZFC and FC susceptibilities when measured in 200 Oe and 500 Oe. The ZFC susceptibility is slightly smaller than the FC susceptibility in both cases. The most interesting is dependence of susceptibility on magnetic field $H$. The susceptibility first increases when the magnetic field is changed from 100 Oe to 200 Oe and 500 Oe. In a field of $H = 500$ Oe the susceptibility has no maximum at 4.6 K and saturates at 2 K as typical for a kind of ferromagnetic transition with multidomain structure within the complex. With still increasing the magnetic field the susceptibility becomes small again (1 kOe and 10 kOe) and for 10 kOe it is well below the value measured in 100 Oe.

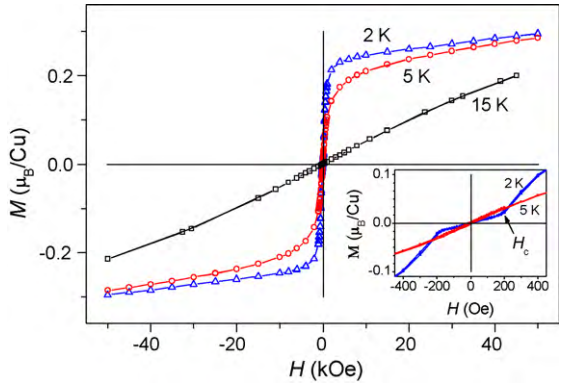


**Fig. 7.** Magnetization as a function of magnetic field at 2 K, 5 K and 15 K for Cu-sample.

In Fig. 7 we show the magnetization as a function of magnetic field $M(H)$ at three temperatures: 15 K, 5 K and 2 K. At 15 K the $M(H)$ is linear up to the maximal field of 50 kOe. We are in the paramagnetic region. At 5 K the steep increase of the magnetization in small magnetic field is followed (from approx. 500 Oe) by the S-shaped curve characteristic for systems with ferromagnetic interactions. This is in agreement with $\chi(T)$ where at 5 K the susceptibility measured in 100 Oe and 200 Oe exhibits a maximum and saturates at 500 Oe. Above 1 T the magnetization slowly and linearly increases up to the 5 T rather than reaching a saturation. The value of magnetization at 50 kOe (0.3 $\mu_B$ per ion $Cu^{2+}$) is still far below the maximum possible magnetization of $\approx 1\ \mu_B/Cu^{2+}$ for $S = 1/2 Cu^{2+}$ ions. Finally, the magnetization at 2 K. In full scale it is very similar to the $M(H)$ at 5 K. The inset in Fig. 7 shows a low-field region for $M(H)$ at 2 K and 5 K. Here we can notice an important difference. At 5 K the $M(H)$ (red curve) is linear with a constant slope up to 500 Oe while at 2 K (the blue curve) magnetization first increases much slower than in 500 Oe (For interpretation of the references to color in this text, the reader is referred to the web version of the article.). At a critical field $H_c = 200$ Oe a "kink" can be observed which means that only high enough magnetic field induces the ferromagnetic behaviour at 2 K. Now we can understand the peculiar susceptibility dependence below 5 K. In magnetic fields below $H_c$ the antiferromagnetic interaction is more effective than the ferromagnetic one and consequently the susceptibilities measured in 100 Oe and 200 Oe are smaller than the susceptibility measured in 500 Oe. No coercitive magnetic field or remanent magnetization were detected at any temperature which is in agreement with the absence of ZFC–FC splitting in $\chi(T)$ curves.

Let us summarize magnetic properties of Cu-complex: above approx. 10 K it is a paramagnet. A weak antiferromagnetic interaction (the negative Curie–Weiss temperature $\Theta$) between neighbour atoms is presents. This antiferromagnetic interaction stays effective below 5 K only in small enough magnetic field. Between 5 K and 2 K and above the critical field $H_c$ that is about 200 Oe at 2 K and vanishes at 5 K the system shows ferromagnetic properties. Ferromagnetic and antiferromagnetic interactions are very tightly connected in our system and it is impossible to deduce a reliable microscopic magnetic structure only from our bulk magnetic measurements. At least in part the observed magnetic properties are similar to the magnetic properties of cobalt(II) with pyromellitate complex [31]. The authors also detected regions in a temperature and magnetic field phase space with different magnetic properties. For the low temperature phase a canted

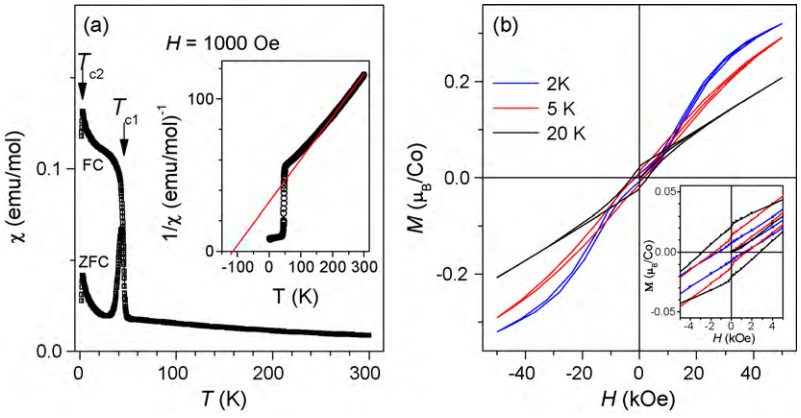


**Fig. 8.** (a) Susceptibility and inverse susceptibility for FC regime (inset) as a function of temperature for the Co-sample. (b) Magnetization as a function of magnetic field at 2 K, 5 K and 20 K.

antiferromagnetism was proposed and maybe this can explain our magnetic data, too. Using the measured magnetization at 2 K in the field of 10 kOe ($M_m$ = 0.25 $\mu_B$/Cu) and the maximal possible saturation magnetization of about $M_0$ = 1 $\mu_B$/Cu for Cu(II) system we obtain from $\sin\alpha = M_m/M_0$ the canting angle $\alpha \approx 14^\circ$. Above 10 kOe the angle only slightly increases as is seen from the gradual increase of magnetization from 10 kOe to 50 kOe.

Fig. 8a shows temperature dependence of susceptibility and inverse susceptibility for $(NH_3OH)_2CoF_4$. In this case $\chi^{-1}$ curve is not linear even in high-temperature region but has a rather parabolic shape. The measured effective moment $\mu_{eff}$ = 5.2 BM at room temperature is just the expected value for noninteracting cobalt(II) ions assuming a spin–orbit coupling in octahedral environment [32]. A negative Curie–Weiss temperature $\Theta \approx -120$ K obtained from $\chi^{-1}$ vs. $T$ graph (inset in Fig. 8a, solid red line) suggests that an antiferromagnetic coupling exists between Co(II) ions at high-temperature (For interpretation of the references to color in this figure legend, the reader is referred to the web version of the article.).

In Co-sample two transitions were observed. Above 50 K there is no difference between ZFC and FC measured susceptibilities. The susceptibility slowly increases from room temperature down to 50 K. At temperature $T_{c1}$ = 46.5 K the susceptibility steep increases and below the $T_{c1}$ the ZFC/FC curves bifurcate. Both observations suggest that ferromagnetic interaction between cobalt(II) ions takes in place at this temperature. Also the hysteresis loop with remanent magnetization of about 0.02 $\mu_B$/Co and coercitive magnetic field of 3 kOe are detected below $T_{c1}$ (Fig. 8b, blue curve measured at 20 K). At the second critical temperature $T_{c2}$ = 3 K an abrupt downturn of the susceptibility indicates an antiferromagnetic interaction. The remanent magnetization and coercitive magnetic field are smaller at $T_{c2}$ and below (Fig. 8b for 5 K and 2 K) as are at 20 K where ferromagnetic interaction was prevailing. Due to the observed hysteresis loops below $T_{c1}$ and antiferromagnetic transition at $T_{c2}$ we tentatively propose a ferrimagnetic order in Co-complex at the lowest temperature rather than canted antiferromagnetism. However we have to notice again that it is hard to deduce an atomic magnetic structure without applying any technique that can probe the magnetic moments of the individual atoms such as for example neutron diffraction experiment.

## 3. Conclusions

In summary, two new hydroxylammonium fluorometalates, $(NH_3OH)_2CuF_4$ and $(NH_3OH)_2CoF_4$, have been synthesized. Both compounds crystallize in monoclinic, $P2_1/c$, space group and are composed of $NH_3OH^+$ cations and $MF_6^{2-}$ anions. Each of $MF_6$ octahedra shares four of its vertices in a way that each vertex is shared between two octahedra resulting in a formation of 2D layers. The title compounds are the first representatives of layered hydroxylammonium fluorometalates. The thermal decomposition of the compounds was studied. The decomposition of $(NH_3OH)_2CuF_4$ takes place in five steps, yielding $Cu_2O$ with traces of CuO. $(NH_3OH)_2CoF_4$ decomposes in two steps, yielding $CoF_2$ after the first step and CoO as the final product. We proposed the chemical reactions for different stages of thermal decomposition by applying qualitative analysis of X-ray powder patterns of polycrystalline products resulting from thermal decomposition at different temperatures and thermogravimetric analysis for both title compounds. Chemical reactions for different stages of thermal decomposition have been proposed on the basis of the thermogravimetric analysis for both title compounds and X-ray powder patterns of decomposition products at different temperatures. High-temperature susceptibilities are consistent with spin-only Cu(II) and Co(II). Both structures exhibit an interesting magnetic behaviour below 50 K where a ferromagnetic and antiferromagnetic interactions are tightly connected. For Cu-complex a canted antiferromagnetic and for Co-complex a ferrimagnetic order was proposed at low temperature.

## 4. Experimental

### 4.1. Materials and methods

Both reactions were carried out in digestorium in air atmosphere. As already reported [15], white crystals of hydroxylammonium fluoride, $NH_3OHF$, were prepared by adding 40% HF dropwise into ethanolic solution of hydroxylammine at 273 K. The white crystals were filtered off, dried and the product was used for further synthesis. Hydroxylammonium was determined by titration [33] with $KMnO_4$ and fluorine with a fluoride-sensitive electrode with direct calibration, using a TISAB IV buffer to provide a constant background ionic strength. Cobalt and copper were determined by gravimetric methods.

### 4.2. Synthesis of $(NH_3OH)_2CuF_4$

After dissolving $CuCO_3 \times Cu(OH)_2$ powder (0.35 g; 1.60 mmol) in 40% HF (3.45 g; 69 mmol), solid $NH_3OHF$ (0.34 g; 6.40 mmol) was added. Blue crystals of $(NH_3OH)_2CuF_4$ were obtained after the evaporation of the solvent at room temperature. The crystals were dried in a dessicator above silica gel (yield 0.29 g, 44.40%). Chemical analysis for $(NH_3OH)_2CuF_4$: 33.34% $NH_3OH^+$ (calc. 32.76%), 29.95% $Cu^{2+}$(calc. 30.62%), 37.22% $F^-$ (calc. 36.62%).

**Table 4**
Crystal data, data collection and refinement summary.

| | $(NH_3OH)_2CuF_4$ | $(NH_3OH)_2CoF_4$ |
|---|---|---|
| *Crystal data* | | |
| $M_r$ | 207.63 | 203.01 |
| Cell setting, space group | Monoclinic, $P2_1/c$ | Monoclinic, $P2_1/c$ |
| Temperature (K) | 293(1) | 293(1) |
| $a$ (Å) | 7.9617(2) | 8.1764(3) |
| $b$(Å) | 5.9527(2) | 5.8571(2) |
| $c$ (Å) | 5.8060(2) | 5.6662(2) |
| $\beta$ (°) | 95.226(2) | 94.675(3) |
| $V$ (Å$^3$) | 274.023(15) | 270.452(17) |
| $Z$ | 2 | 2 |
| $D_x$ (Mg m$^{-3}$) | 2.516 | 2.493 |
| Radiation type | Mo $K\alpha$ | Mo $K\alpha$ |
| $\mu$ (mm$^{-1}$) | 4.011 | 3.198 |
| Crystal form, colour | Blue prism | Violet stick |
| Crystal size (mm) | $0.1 \times 0.2 \times 0.3$ | $0.1 \times 0.1 \times 0.015$ |
| *Data collection* | | |
| Diffractometer | Nonius Kappa CCD | Nonius Kappa CCD |
| Data collection method | ω scan | ω scan |
| Absorption correction | Multiscan | Multiscan |
| No. of measured, independent and observed reflections | 7675, 801, 730 | 5308, 781, 663 |
| Criterion for observed reflections | $F^2 > 2.0\sigma(F^2)$ | $F^2 > 2.0\sigma(F^2)$ |
| $R_{int}$ | 0.045 | 0.037 |
| $\theta$ range (°) | 1.00–30.03 | 1.00–30.03 |
| $h$ range | $-11 \rightarrow 11$ | $-11 \rightarrow 11$ |
| $k$ range | $-8 \rightarrow 8$ | $-8 \rightarrow 8$ |
| $l$ range | $-8 \rightarrow 8$ | $-7 \rightarrow 7$ |
| *Refinement* | | |
| Refinement on | $F$ | $F$ |
| $R$ (on $F_{obs}$), $wR$ (on $F_{obs}$), $S$ | 0.030, 0.021, 1.772 | 0.026, 0.023, 0.718 |
| No. of contributing reflections | 771 | 737 |
| No. of parameters | 59 | 59 |
| H-atom treatment | Obtained from difference Fourier map; refined with isotropic displacement parameters | Obtained from difference Fourier map; refined with isotropic displacement parameters |
| $(\Delta/\sigma)_{max}$, $(\Delta/\sigma)_{ave}$ | 0.0002, 0.0002 | 0.0009, 0.0001 |
| $\Delta\rho_{max}$, $\Delta\rho_{min}$ (eÅ$^3$) | 0.627, −1.3 | 0.453, −0.746 |

### 4.3. Synthesis of $(NH_3OH)_2CoF_4$

Co powder (0.20 g, 3.40 mmol) was dissolved in hot 40% HF (3.45 g; 69 mmol) and heated for 8 min. After cooling to room temperature, solid $NH_3OHF$ (0.36 g; 6.80 mmol) was added. Violet crystalline phase was obtained in about 5 days after the evaporation of the solvent at room temperature. The crystals were dried in a dessicator above silica gel (yield 0.31 g, 66.67%). Chemical analysis for $(NH_3OH)_2CoF_4$: 35.03% $NH_3OH^+$ (calc. 33.51%), 29.26% $Co^{2+}$(calc. 29.04%), 37.05% $F^-$ (calc. 37.45%).

### 4.4. Methods of characterisation

Thermogravimetric analysis was carried out on a METTLER TGA/SDTA851$^e$ system in the temperature range 35–1000 °C (TG) and 37–400 °C (DSC) in nitrogen flow (100 ml/min) with a heating rate of 10 K/min, using $Al_2O_3$ crucibles.

X-ray powder diffraction data were collected with an AXS Bruker/Siemens D5005 diffractometer using $CuK_{\alpha 1}$ radiation at 293 K. The samples were finely ground, placed on a silicone-crystal holder and measured in the range $10^\circ < 2\Theta < 70^\circ$ with a step 0.0144° and a scanning speed of 5 s/step. The obtained data were analyzed using the EVA program and the PDF datafile [34].

### 4.5. Magnetic measurements

The magnetic properties of the two compounds were measured using a Quantum Design MPMS-XL-5 susceptometer equipped with a SQUID detector. The data were collected between 2 K and 300 K in several magnetic fields and isothermal magnetizations were measured between 50 kOe and 50 kOe.

### 4.6. X-ray structure determination

Diffraction data for the single crystals of both compounds have been collected on a Nonius Kappa CCD diffractometer at room temperature (293 ± 2 K) with $MoK_\alpha$ radiation and graphite monochromator. The data were processed using DENZO program [35]. Structures were solved by direct methods using SIR97 [36]. A full-matrix least-squares refinement on $F$ was employed with anisotropic temperature displacement parameters for all non-hydrogen atoms and isotropic for hydrogen atoms.

XTAL3.6 program suite [37] was used for structure refinement and interpretation. Figs. 4 and 5 were produced using ORTEP-3 [38] and ATOMS [39], respectively. Further details of crystal data, data collection and refinement can be found in Table 4. Further details of the crystal structure investigations may be obtained from the Fachinformationszentrum Karlsruhe, 76344 Eggenstein-Leopoldshafen, Germany, on quoting the depository numbers CSD-421615 and CSD-421616.

## Acknowledgement

The authors thank for the support of the Ministry of Higher Education, Science and Technology of the Republic of Slovenia.

## References

[1] E. Ebler, E. Schott, J. Prakt. Chem. 78 (1908) 338–340.
[2] B. Sahoo, D. Patnaik, Curr. Sci. 30 (1961) 293–296.
[3] B. Frlec, H.H. Hyman, Inorg. Chem. 12 (1967) 2233–2239.
[4] M. Pintarič, S. Milićev, B. Volavšek, Monatsh. Chem. 121 (1990) 357–360.
[5] M. Kristl, B. Volavšek, L. Golič, Monatsh. Chem. 127 (1996) 581–586.
[6] I. Ban, M. Kristl, B. Volavšek, L. Golič, Monatsh. Chem. 130 (1999) 401–408.

[7] M. Kristl, I. Ban, M. Drofenik, A. Popović, J. Fluorine Chem. 109 (2001) 209–212.
[8] M. Kristl, M. Drofenik, L. Golič, Acta Chim. Slov. 49 (2002) 243–250.
[9] I. Ban, M. Kristl, M. Drofenik, A. Popović, Thermochim. Acta 419 (2004) 253–257.
[10] I. Bajc, S. Milićev, B. Volavšek, Monatsh. Chem. 123 (1992) 321–324.
[11] I. Ban, L. Golič, S. Milićev, B. Volavšek, Monatsh. Chem. 126 (1995) 1279–1289.
[12] I. Ban, B. Volavšek, L. Golič, Z. Anorg. Allg. Chem. 628 (2002) 695–698.
[13] M. Kristl, M. Drofenik, L. Golič, A. Golobič, Acta Chim. Slov. 50 (2003) 431–440.
[14] B. Dojer, M. Kristl, Z. Jagličić, M. Drofenik, A. Meden, Acta Chim. Slov. 55 (2008) 834–840.
[15] M. Kristl, L. Golič, B. Volavšek, Monatsh. Chem. 125 (1994) 1207–1213.
[16] H.M. Haendler, F.A. Johnson, D.S. Crocket, J. Am. Chem. Soc. 80 (1958) 2662–2664.
[17] D.S. Crocket, R.A. Grossman, Inorg. Chem. 3 (1964) 644–646.
[18] S.I. Troyanov, I.V. Morozov, Y.M. Korenev, Zhurn. Neorgan. Khimii 38 (1993) 984–989.
[19] S. Troyanov, Y. Morozov, L. Kholodkovskaya, Russ. J. Inorg. Chem. (Engl. Transl.) 35 (1990) 1758–1764.
[20] H. Siebert, B. Breitenstein, Z. Anorg. Allg. Chem. 379 (1970) 44–47.
[21] M.N. Bhattacharjee, M.K. Chaudhuri, M. Devi, Polyhedron 11 (1992) 1523–1529.
[22] E. Herdtweck, D. Babel, Z. Anorg. Allg. Chem. 474 (1981) 113–122.
[23] R. Haegele, D. Babel, Z. Anorg. Allg. Chem. 409 (1974) 11–22.
[24] D. Reinen, S. Krause, Inorg. Chem. 20 (1981) 2750–2759.
[25] K. Knox, J. Chem. Phys. 30 (1959) 991–993.
[26] M. Hidaka, K. Inoue, I. Yamada, P.J. Walker, Phys. B and C 121 (1983) 343–350.
[27] L.J. Farrugia, J. Appl. Crystallogr. 30 (1997) 565.
[28] D. Babel, E. Herdtweck, Z. Anorg. Allg. Chem. 487 (1982) 75–84.
[29] M. Welsch, D. Babel, Zeitschr. Naturforsch. B 46 (1991) 161–164.
[30] J.H. Van Vleck, Theory of Electric and Magnetic Susceptibilities, Oxford University Press, Oxford, 1932, pp. 285.
[31] H. Kumagai, C.J. Kepert, M. Kurmoo, Inorg. Chem. 41 (2002) 3410–3422.
[32] F.E. Mabbs, D.J. Machin, Magnetism and Transition Metal Complexes, Chapman and Hall Ltd., London, 1973.
[33] N.H. Fuhrmann, 6th ed, Standard Methods of Chemical Analysis, vol. 1, Van Nostrand, Princeton, NJ, 1962, pp. 362.
[34] DIFFRAC$^{plus}$ Search/Match, Version 3.0, PDF1, PDF2, 1997.
[35] Z. Otwinowski, W. Minor, Methods Enzymol. 276 (1997) 307–326.
[36] A. Altomare, M.C. Burla, M. Camalli, G. Cascarano, C. Giacovazzo, A. Guagliardi, A.G.G. Moliterni, G. Polidori, R. Spagna, J. Appl. Crystallogr. 32 (1999) 115–119.
[37] S.R. Hall, D.J. Du Boulay, R. Olthof-Hazekamp (Eds.), Xtal3. 6 System, University of Western Australia, Lamb, Perth, 1999.
[38] R. Minkwitz, H. Preut, M. Seifert, D. Lamek, Zeitschr. Naturforsch. B 48 (1993) 1241–1247.
[39] E. Dowty, ATOMS, Version 6.2. Shape Software, Kingsport, USA, 2005.